On Directional Measurement Representation in Orbit Determination

Evan M. Ward and Greg Carbott

U.S. Naval Research Lab, Washington, DC 20375

Precision Orbit Determination (OD) is often critical for successful satellite operations supporting a wide variety of missions. Directional or angles only measurements of a satellite are typically represented in spherical coordinates on the observer's celestial sphere (e.g. azimuth and elevation or right ascension and declination). Computing residuals in these angular coordinates during the OD process can introduce errors in the same way an equirectangular projection distorts both distance and direction on a map. One technique is to weight the azimuth residuals by the cosine of the elevation, as in a sinusoidal projection. While this technique preserves the length of every parallel it still induces distortion in direction and distance. Therefore, it is proposed to use the angular distance between the computed and observed locations as the residual. This is similar to using an azimuthal equidistant projection with the observed location at the center. It is shown that this technique removes distortion present in the other two representations. The three techniques are then compared experimentally for a geostationary and a low Earth orbit satellite using simulated data to evaluate their differences. It is shown that using angular distance as the residual decreases the number iterations required for convergence and allows the OD process to more closely fit the observed data when there are observations near the pole of the spherical coordinate representation.

I.   Introduction

Accurate Orbit Determination (OD) is often critical for successful satellite operations supporting a wide variety of missions. Precision OD involves accurately modeling all satellite observations, including angular or directional observations such as those obtained from astrometry. Standard methods for OD, the Kalman Filter (KF) and Weighted Least Squares (WLS), assume a Gaussian distribution for the observations and then attempt to find the Maximum Likelihood Estimate (MLE). Therefore the choice of observation representation has a significant effect on the size and shape of the likelihood function which it turn affects the MLE. Other work on representation in OD has focused on the estimated state where Junkins et. al.[1] found the choice of state representation has a significant effect on the shape and characteristics of the estimated covariance.

Standard OD references suggest representing directional measurement as azimuth and elevation; right ascension and declination; North-South and East-West angles; or some other representation of direction in spherical coordinates.[2–6] An orbit determination manual by Kuga and Gill[7] describes a process of converting angular measurements to a unit vector to apply refraction and then converting back to spherical coordinates for computing the residuals. Similarly the Goddard Trajectory Determination System (GTDS) mathematical theory[8] uses spherical coordinates representation for direction measurements. Several recently published works on OD compute residuals in spherical coordinates as well.[9, 10] The Naval Research Laboratory's (NRL) Orbit Covariance Estimation and Analysis (OCEAN) OD application weights azimuth residuals by the cosine of the corresponding elevation angle to account for the convergence of meridians near the poles.[11] None of these references suggest using angular distance on the celestial sphere as the residual as is recommended in this paper.

Choosing a representation for directional measurements is equivalent to choosing a transformation from location on a sphere to location in a plane which has a long history in map making. Using a point's spherical coordinates as its planar coordinates is known as the equirectangular or plate carrée projection. While simple to construct, it is problematic because of its distortion in angle and distance, especially near the poles.[12] Weighting longitude by the cosine of latitude is the sinusoidal projection which has "no distortion along the

American Institute of Aeronautics and Astronautics

Equator and central meridian, but distortion becomes pronounced near the outer meridians, especially in the polar regions."[12] The azimuthal equidistant projection, a projection that is often used for air navigation, preserves distance and direction from the central point.[12] The distortion caused by the chosen projection changes how the OD process computes distance (residual) and direction (gradient) between observed and computed measurements.

In the following section, three direction observation representations are defined and compared analytically. The three representations are spherical coordinates, weighted spherical coordinates, and a unit vector based approach. Then Section III describes a method for comparing the representations using simulated data for a Low Earth Orbit (LEO) and a Geostationary Earth Orbit (GEO) satellite. Section IV discusses the results from the numerical simulations and finally Section V presents the authors' conclusions.

II.   Direction Representation

The choice of direction representation affects not only the size of the residual but also the shape of the assumed probability distribution since in WLS OD or KF OD the observations are assumed to be samples of a Normal distribution. For the OD solution to be the Maximum Likelihood Estimate (MLE), the cost function must have the same shape as the probability distribution of the observations. For this paper it is assumed observations are Normally distributed about the true point on the celestial sphere, the distribution is symmetric about the true point and the distribution is independent of location on the celestial sphere.

All angular direction representations incur some error because the domain of the Normal distribution is infinite but the range of any angular measurement is at most 2π, though this limitation is minimal when the limits are many standard deviations away from the evaluated point. A potentially larger concern is the local distortion in shape and distance caused by the choice of projection from the sphere to the plane. The following discussions examine three different direction representations that correspond to the the plate carrée, sinusoidal and azimuthal equidistant projections.

Spherical Coordinates

The first approach is directly using spherical coordinates where direction is represented as a pair of angles such as azimuth and elevation; longitude and latitude; or right ascension and declination. The following discussion uses azimuth and elevation though mathematically these systems are equivalent, differing only in the choice of reference planes. Residuals formed in spherical coordinates take the form

$$r_\alpha = \alpha_c - \alpha_o = \Delta\alpha \tag{1}$$
$$r_\varepsilon = \varepsilon_c - \varepsilon_o = \Delta\varepsilon \tag{2}$$

where r is the residual, α is the azimuth angle, ε is the elevation angle, subscript o denotes observed and subscript c denotes computed. The corresponding cost function to be minimized in the OD process is

$$C_s = r_\alpha^2 + r_\varepsilon^2 = (\Delta\alpha)^2 + (\Delta\varepsilon)^2. \tag{3}$$

This cost function is analogous to using an equirectangular projection. Though effective near zero elevation, the azimuth residuals can be large for small differences in direction near the poles ($\varepsilon = 90°$).

Weighted Spherical Coordinates

The second approach is to preserve area in mapping the celestial sphere to the plane by weighting the azimuth residual by the length of the corresponding small circle of constant elevation,

$$C_w = (\Delta\alpha \cos\varepsilon_o)^2 + (\Delta\varepsilon)^2 \tag{4}$$

which is similar to the sinusoidal projection. While this projection preserves area, it does not, in general, preserve distance or direction between points. This has the effect of de-weighting azimuth observations near the poles. In the extreme case where there are many observations at high elevation this representation can reduce the observation set by half by eliminating the azimuth observations.

Unit Vectors

A third, alternative representation can be derived from using unit vectors to represent directions. The angle between the observed and computed directions can be used as the residual.

$$r_\theta = \theta \tag{5}$$

The angle between two vectors can be computed either from the dot product

$$\cos\theta = \mathbf{u}_c \cdot \mathbf{u}_o \tag{6}$$

or the cross product

$$\sin\theta = |\mathbf{u}_c \times \mathbf{u}_o| \tag{7}$$

where $\mathbf{u}$ is a unit vector. Though mathematically equivalent, Equation 7 is preferred for computer implementation because the dot product is insensitive to changes when θ is small. The unit vector derived cost function is

$$C_u = \theta^2. \tag{8}$$

While Equation 8 effectively measures the angular distance between observed and computed points it only provides one equation per direction observation. A second angular equation can be added to keep two independent equations per direction observation by measuring the angle out of the $\mathbf{u}_c$, $\mathbf{u}_o$ plane. First define the normal to the plane

$$\mathbf{u}_n = \mathbf{u}_c \times \mathbf{u}_o \tag{9}$$

then

$$\sin\phi = \mathbf{u}_c \cdot \mathbf{u}_n \tag{10}$$

defines the out of plane angle and $r_\phi = \phi$ is the residual. When differentiating Equation 10 $\mathbf{u}_n$ is treated as a constant since it is defining a new frame. The residual r_ϕ does not contribute to the cost or its derivative because it is always zero. In this way the unit vector approach can be viewed as defining a new system of spherical coordinates for every computed point with $\mathbf{u}_c$ and $\mathbf{u}_o$ defining the equatorial plane.

Comparison

In general, the three approaches produce different results. However, under certain assumptions C_u is shown to be equivalent to C_w and C_w is shown to be equivalent to C_s. This result is used Section III to design experiments that show the differences and similarities between the methods.

For small values of θ, $\Delta\alpha$ and $\Delta\varepsilon$ C_u is equivalent to C_w. Using the small angle approximation and Equation 7

$$\theta = |\mathbf{u}_c \times \mathbf{u}_o|. \tag{11}$$

Expressing each unit vector in spherical coordinates and taking the magnitude of the cross product gives

$$C_u = \theta^2 = (\mathrm{s}\,\alpha_c\,\mathrm{s}\,\varepsilon_o\,\mathrm{c}\,\varepsilon_c - \mathrm{s}\,\alpha_o\,\mathrm{s}\,\varepsilon_c\,\mathrm{c}\,\varepsilon_o)^2 + (\mathrm{s}\,\varepsilon_c\,\mathrm{c}\,\alpha_o\,\mathrm{c}\,\varepsilon_o - \mathrm{s}\,\varepsilon_o\,\mathrm{c}\,\alpha_c\,\mathrm{c}\,\varepsilon_o)^2 + \mathrm{s}^2\,(\alpha_c - \alpha_o)\,\mathrm{c}^2\,\varepsilon_c\,\mathrm{c}^2\,\varepsilon_o \tag{12}$$

where s and c denote sine and cosine respectively. Substituting $\alpha_c = \alpha_o + \Delta\alpha$, $\varepsilon_c = \varepsilon_o + \Delta\varepsilon$, and ignoring term of order greater than two results in

$$C_u = (\Delta\alpha)^2 \cos^2\varepsilon_o + (\Delta\varepsilon)^2 \tag{13}$$

which is Equation 4. Therefore, it is also true that the derivatives C_u are equivalent to the derivatives of C_w when θ, $\Delta\alpha$, and $\Delta\varepsilon$ are all small.

For small values of ε_o C_w is equivalent to C_s. Using the approximation that $\cos\varepsilon_o \approx 1$

$$C_w = (\Delta\alpha)^2 + (\Delta\varepsilon)^2$$

which is the definition of C_s in Equation 3. Therefore, when θ, $\Delta\alpha$, $\Delta\varepsilon$, and ε_o are all small the three methods are equivalent.

While spherical and unit vector based representations are the same for small angles they produce different results when any one of three angles (θ, $\Delta\alpha$, or $\Delta\varepsilon$) is large. For large angles C_u still accurately measures

distance on the celestial sphere because that is its definition, but C_w and C_s do not because they are not equivalent to C_u for large angles. Large residuals may occur when the initial guess of the satellite's orbit is far from its actual orbit, as is common in initial OD scenarios. The distortion caused by using a spherical representation is hypothesized to cause slow convergence or cause divergence.

When the initial guess is accurate, θ and $\Delta\varepsilon$ are small but $\Delta\alpha$ may still be large when there are observations near the pole of the spherical representation. An example is illustrated in Figure 1 where $\theta \leq 5°$ only implies $\Delta\alpha \leq 90°$ which is quite large. From the figure it is apparent that there are significant differences between the cost functions, i.e. assumed error distributions, imposed by the different representations. C_w favors lower elevations than C_u and C_s is much thinner in azimuth, hence emphasizing azimuth measurements more than the other two cost functions. Since the gradient is normal to the level curves shown in Figure 1 it is also evident there are significant differences in the derivatives. For example, near the cusp of C_w at $\varepsilon = 90°$ the gradient is normal to the direct great circle path to $\mathbf{u}_c$. As well as causing slow convergence, the differences in the cost function may cause the OD process to converge to different solutions. It is hypothesized that using a unit vector representation leads to more accurate OD than using a spherical coordinate representation when there are observations very close to the pole.
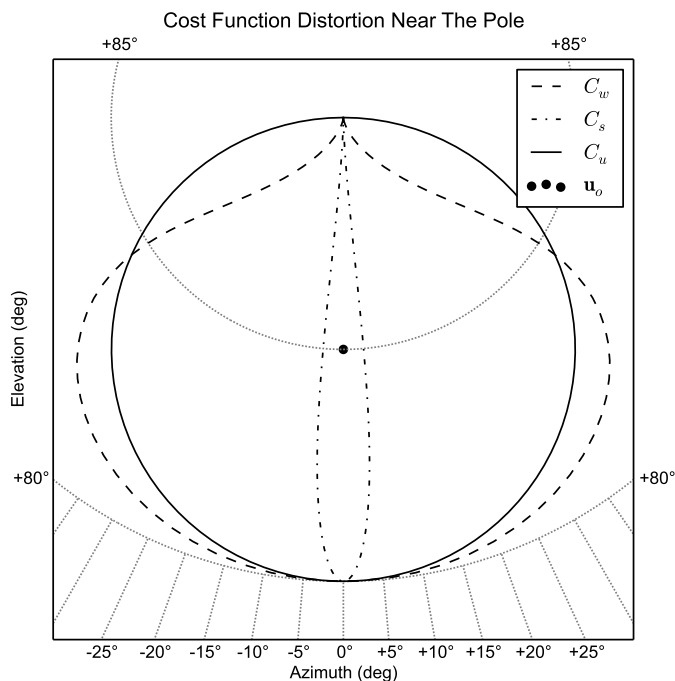

Figure 1: Level curves of the three cost functions near the poles showing an example of the distortion caused by using different direction representations. The figure uses an azimuthal equidistant projection centered on the observed direction. Each level curve is plotted for the value $C = (5°)^2$.

III.   Method

The three direction representations are tested with simulated data using a NRL WLS OD software program called State Estimation Application, or SEA. This tool is written in Java using the Orekit[a] space dynamics library and Hipparchus[b] mathematics library. SEA is used at NRL for OD research and is compared to NRL's operational OD application, OCEAN, in a previous paper.[13]

Each representation is tested for a Low Earth Orbit (LEO) and a Geostationary Earth Orbit (GEO) satellite with the initial orbital parameters shown in Table 1. Different ground sites are used for the LEO and

---

[a]https://orekit.org/
[b]https://www.hipparchus.org/

Table 1: Orbital Parameters for the LEO and GEO satellite

Parameter	LEO	GEO
Semimajor Axis	6878.14 km	42,166.3 km
Eccentricity	0	0
Inclination	45 deg	0.01 deg
Argument of Perigee	0 deg	0 deg
Lon. of Ascending Node	235.929 deg	30.018 deg
True Anomaly	0 deg	360 deg

Table 2: Ground Stations used for LEO and GEO satellites

	GS-LEO	GS-GEO
Latitude	38.9 N deg	0.0 deg
Longitude	77.0 W deg	30.0 deg
Altitude	0 km	0 km

GEO test cases as shown in Table 2. The LEO test cases are designed to evaluate the different representations when all three are expected to have similar performance since for LEO satellite passes most of the data has low elevation angles. The GEO satellite's orbit is chosen to evaluate an extreme case where all observations are close to the pole.

Truth ephemerides are produced in Systems Took Kit (STK) using its High-Precision Orbit Propagator (HPOP). STK is used instead of SEA to produce the truth ephemeris so that different implementation of the force force and measurement models are used during OD. Both truth ephemerides include the WGS84 - EGM96 gravity model, ocean tides, and Sun & Moon third body gravity. The GEO ephemeris includes solar radiation pressure. The same force models were included in SEA during OD to maintain consistency.
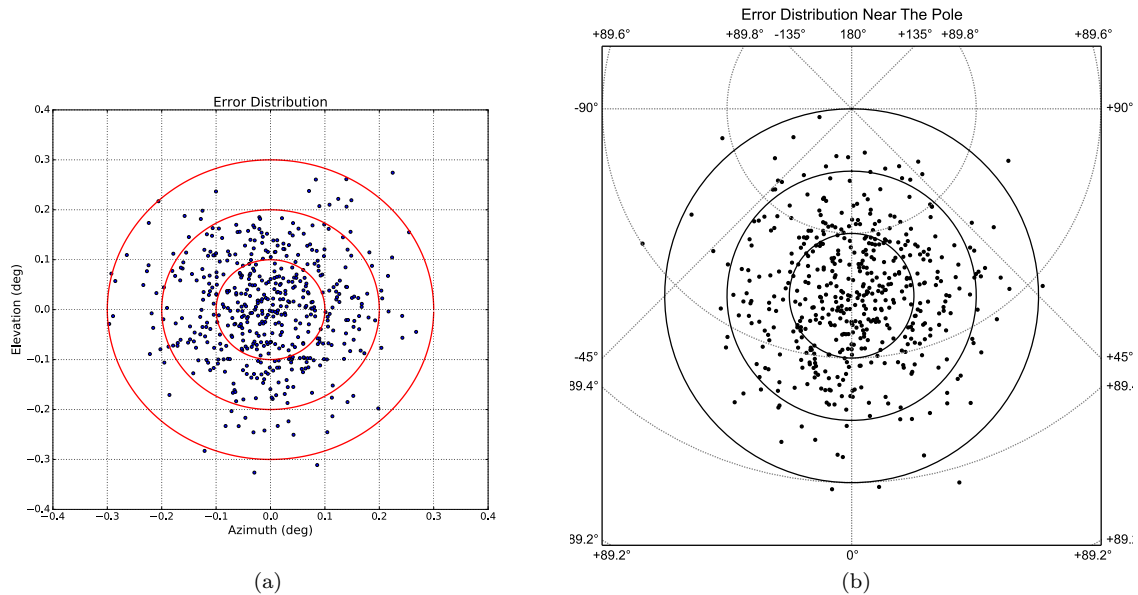

(a)

(b)

Figure 2: Observation error distribution with samples at two example points. Each plotted circle has a radius of 1, 2, and 3 times the standard deviation. The plot on the left is centered at 0° azimuth 0° elevation and the plot on the right is centered at 0° azimuth 89.7° elevation.

The truth ephemeris is used to create simulated input observations for SEA. Noise is added to the direction observations such that the distribution is symmetric about the observed direction and is independent of the observed direction's location on the celestial sphere. Noise is Normally distributed with a standard deviation of 0.1 degree. The distribution is shown for two example points in Figure 2.

The LEO test cases have observations that consist of several passes over a given day as shown in Table 3.

American Institute of Aeronautics and Astronautics

Table 3: LEO Observations

Pass Number	Start Time (UTC)	Duration (min)	Max Elevation (deg)	Used in LEO Test Case 2
P-1	00:11	9.68	79.43	√
P-2	01:50	9.29	36.51	
P-3	03:30	9.22	35.05	
P-4	05:09	9.61	88.38	√
P-5	06:48	7.57	16.57	
P-6	22:09	7.33	14.97	
P-7	23:46	9.68	80.63	√

All seven of the passes are used in the first LEO test case, while only the passes that have a high maximum elevation angle were are in the second LEO test case. The LEO ground station is set to have an elevation mask of 5 degrees. The observations are generated every 10 seconds.

The GEO test cases have observations spanning an entire day with a time step of 30 seconds. The first GEO test case uses every observation for a total of 2880 data points. The second GEO test case uses the same set of observations, but has several black-out periods of 1-2 hours to evaluate the different representations performance with a reduced data set. The total number of observations used in the this case is 1500.

Once generated, the observations are processed by SEA using a separate measurement model for each direction representation. In each case the weights are set appropriately for a standard deviation of 0.1 degrees. SEA uses a Levenburg-Marquardt optimizer and the convergence criteria is a change in the weighted RMS residuals of 10^{-6} or less.

Table 4: The magnitude of the initial condition offset from truth.

Case	IC-1	IC-2	IC-3	IC-4
LEO	214.0 km	420.1 km	886.8 km	395.4 km
GEO	153.9 km	35.9 km	10.2 km	8.1 km
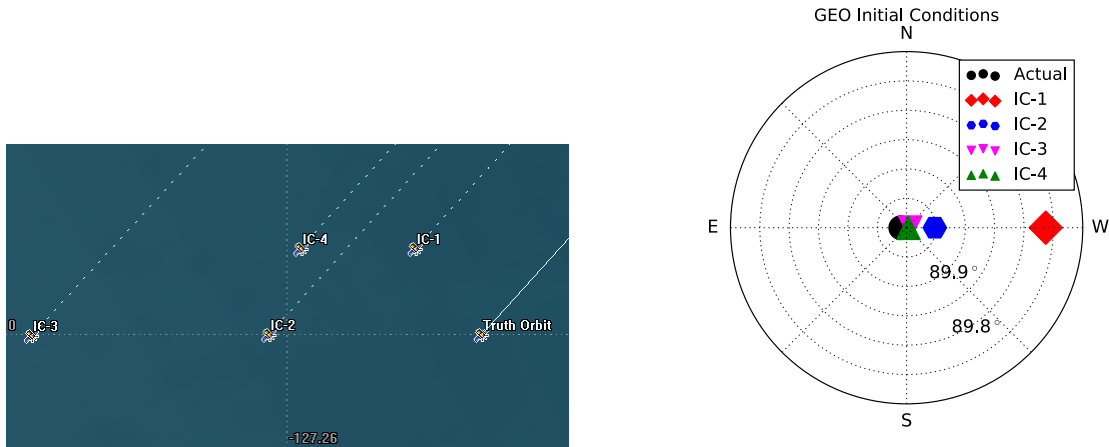
(a) Snapshot of LEO ICs. The truth orbit is located on the far right.

(b) View of the GEO ICs as seen from the ground station.

Figure 3: Initial Conditions for OD.

A single run evaluates a single direction representation with a set of observations and a given initial condition. For each initial condition three runs are performed, one with each direction representation. A test case consists of using four different initial conditions with the same observation set. The initial conditions are shown in Table 4 and graphically in Figure 3. The initial conditions are chosen to evaluate the different representations for different magnitudes of the initial resdiuals. For each satellite one test case is run with

American Institute of Aeronautics and Astronautics

all the observations and then a second test case is run with the reduced set of observations, for a total of four test cases.

IV. Results

The direction representations are evaluated based on two criteria: the difference between estimated and truth ephemerides during the fit span, and the number of iterations to convergence. The ephemeris difference is computed as the RMS of the magnitude of the position difference at every point during the fit span.
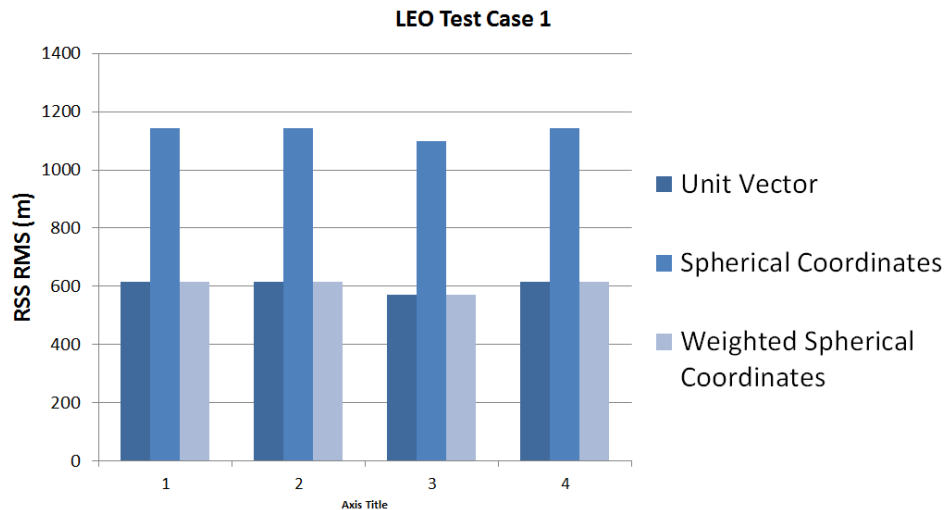
LEO Test Cases

Figure 4: LEO test case 1 ephemeris difference.
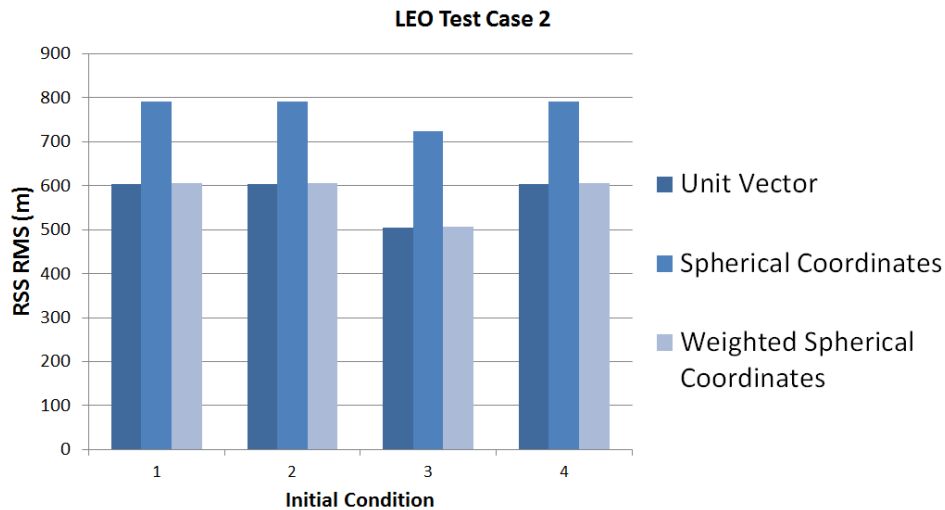
Figure 5: LEO test case 2 ephemeris difference.

Ephemeris differences for the LEO test cases are shown in Figures 4 and 5. In all cases the weighted spherical coordinates representation and the unit vector representation converge to nearly the same solution, differing by up to 0.2% in the estimated ephemeris's distance from the truth ephemeris. The spherical coordinates representation always converges to a solution farther from the truth than the other two representations. The spherical coordinates representation has a RMS at least 1.8 times greater than the other representations

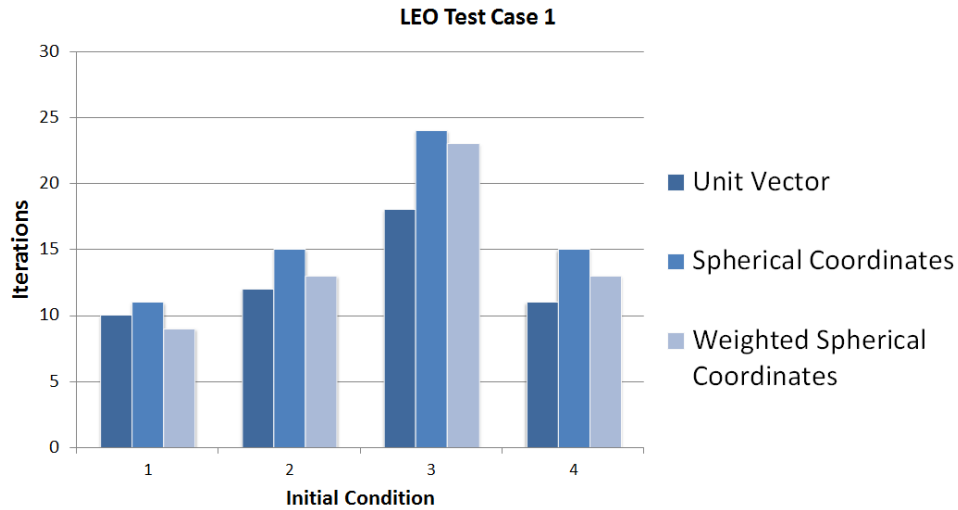American Institute of Aeronautics and Astronautics

Figure 6: The number of iterations until convergence for the first LEO test case.
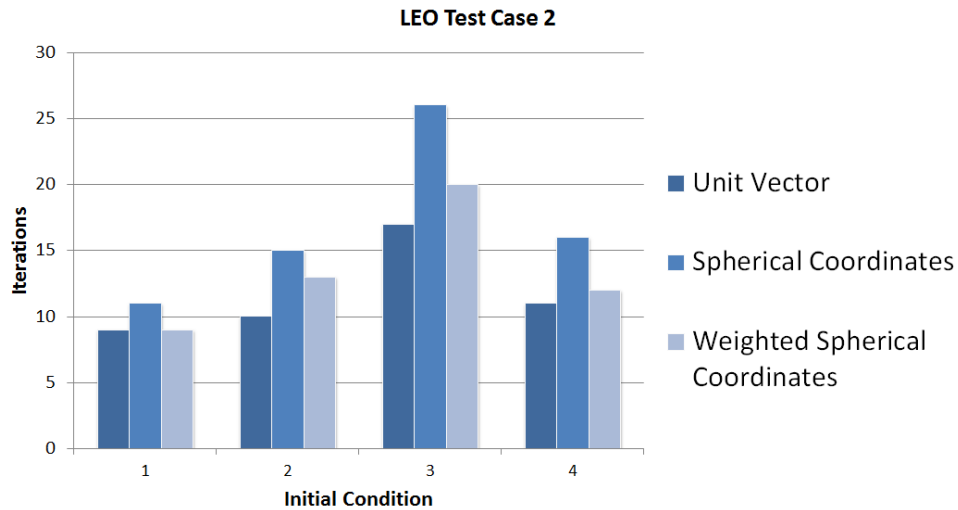

Figure 7: The number of iterations until convergence for the second LEO test case.

in LEO test case 1 and at least 1.3 times greater in LEO test case 2. When starting from IC-3, the furthest initial condition, each representation converges to a different solution than when started from the other three initial conditions. This suggests multiple local optima exist and that the initial condition determines which is selected.

The number of iterations for each method are shown in Figures 6 and 7. Spherical coordinates representation uses more iteration than the other two representations in every case. Unit vector representation converges in fewer iterations than weighted spherical coordinates representation in six out of the eight cases examined. Reducing the amount of data does not seem to have a significant effect on the number of iterations until convergence. Another trend is that all methods converge the quickest using IC-1, which is the closest to the truth, and slowest using IC-3, which is the farthest.

GEO Test Cases

Compared to the other methods the unit vector representation produces an estimate with the smallest ephemeris difference as shown in Figures 8 and 9. The RMS ephemeris difference for the unit vector representation is 3.418 km in GEO test case 1 and 3.187 km in GEO test case 2 for all initial conditions tested.
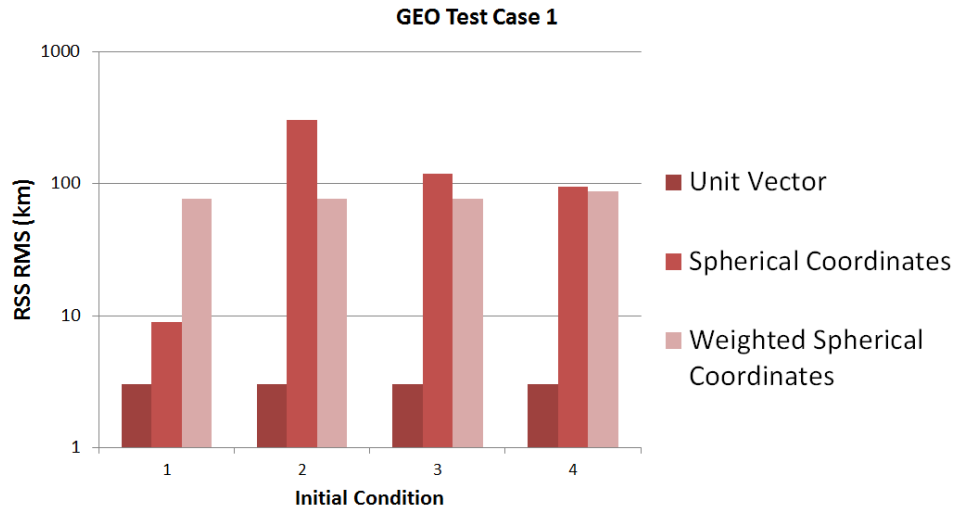
American Institute of Aeronautics and Astronautics

Figure 8: GEO test case 1 ephemeris difference.
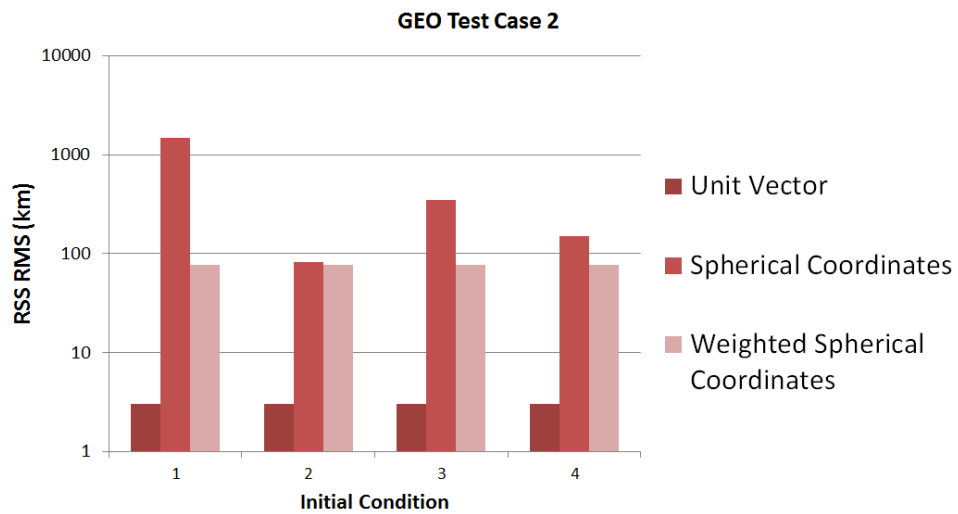
Figure 9: GEO test case 2 ephemeris difference.

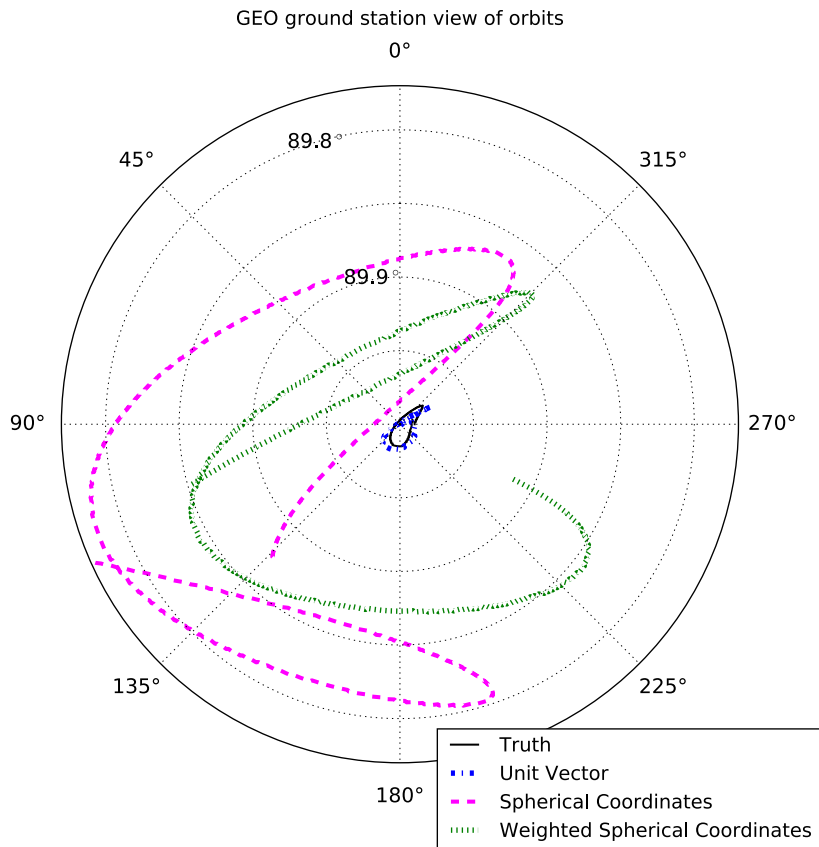American Institute of Aeronautics and Astronautics

Figure 10: The truth orbit and three orbit solutions each determined using a different direction representation as seen from the GS ground station point of view.

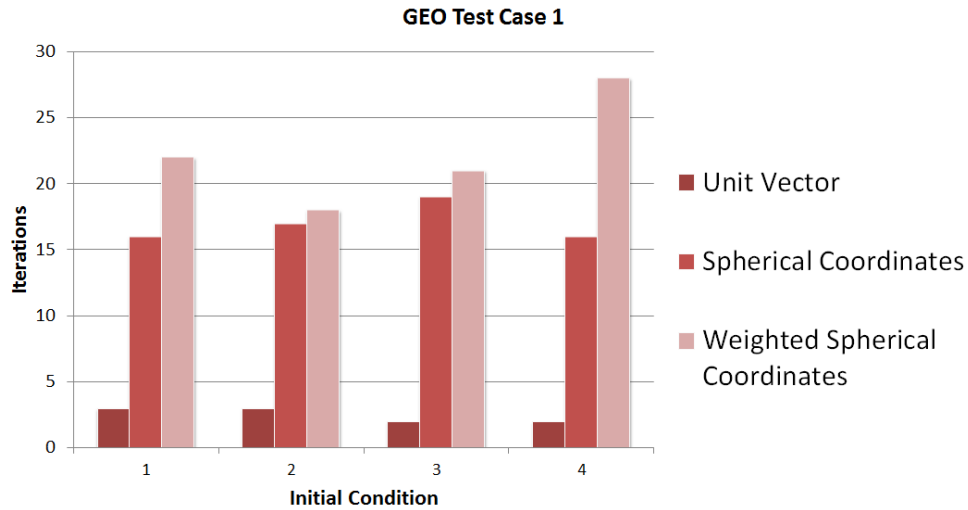American Institute of Aeronautics and Astronautics

Figure 11: The number of iterations until convergence for the first GEO test case.
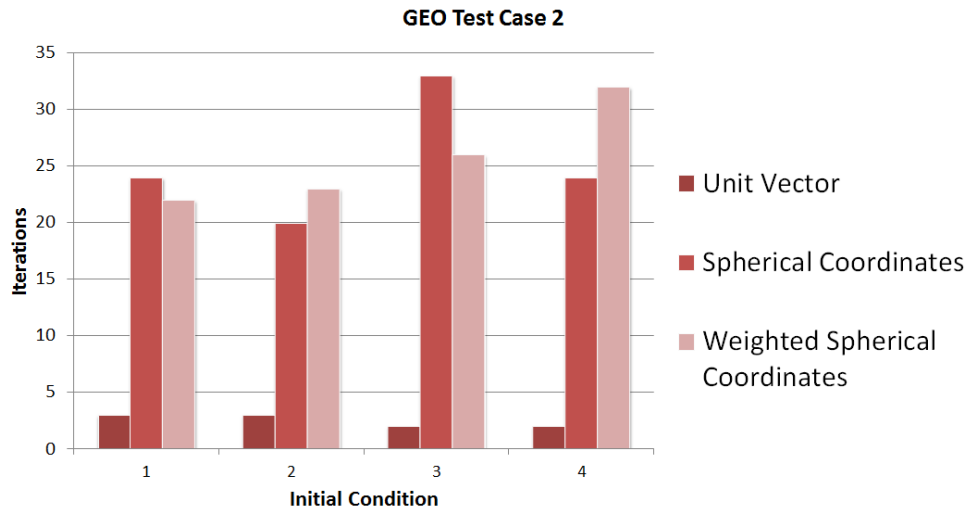

Figure 12: The number of iterations until convergence for the second GEO test case.

This implies the unit vector representation converges to the same solution regardless of initial condition. The unit vector representation achieves a lower RMS ephemeris difference than the other two representations by a factor of at least 2.6 in all test cases. The greatest difference appears in test case 1 IC-2 where the ephemeris difference for the unit vector representation is 47.3 times smaller than the spherical coordinates representation. Additionally, spherical coordinates representation leads to significant variation in the solution while the other two representations consistently converge to the same solution. Figure 10 shows the truth orbit of the GEO satellite as well as solutions using the three different methods from the ground station's point of view, illustrating the differences in solution accuracy. In the figure the estimate from the unit vector representation is almost indistinguishable from the truth ephemeris. The solutions shown are from GEO test case 1, IC-3.

The unit vector method converges within 3 iterations for each IC in both GEO test cases which is fewer than then other methods as shown in Figures 11 and 12. Even with fewer observations, the unit vector method was able to converge to a solution using the same number of iterations. The two other methods took longer to converge when there were fewer observations within the fit span. In all except for GEO test case 2 IC-1, the weighted spherical coordinates representation took a few iterations longer to converge than the unweighted spherical coordinates representation.

American Institute of Aeronautics and Astronautics

Discussion

The first hypothesis, that the unit vector representation converges quicker when the errors in the initial condition are large, is confirmed. In the GEO test cases IC-1 is the farthest initial condition and the unit vector representation converges quicker than the other methods by at least 13 iterations. For the LEO test cases IC-3 is the farthest and the unit vector representation converges quicker than the other methods by at least three iterations. When the errors in the initial condition are small, as for LEO IC-1, unit vector representation uses the same number of iterations or one more iteration than weighted spherical coordinates representation.

The second hypothesis, that using the unit vector representation produces a more accurate solution in the presence of high elevation observations, is confirmed in the GEO case where all observations are above 89 degrees elevation. The unit vector approach improves solution accuracy by more than an order of magnitude while reducing the number of iteration by more than a factor of five. This result is partly due to the distortion caused by weighted and un-weighted spherical coordinate representation at high elevation angles. This result is also partly due to the assumed probability distribution in elevation extending beyond the physical bounds of the elevation angle when using a weighted or un-weighted spherical coordinates representation. While a physics based elevation distribution has zero probability of $\varepsilon > 90°$ the assumed distribution places significant probability on non-physical elevation angles, leading to a less accurate solution. In the weighted spherical coordinates representation the azimuth observations are effectively deleted from the dataset by assigning them a near zero weight which reduces the dataset by half. In the unweighted spherical coordinates representation far too much emphasis is placed on azimuth observations which appears to cause the OD process to fit some of the noise in the observations. Both spherical coordinates representations are unable to average the remaining elevation observations to 90° because the average elevation angle in the input data is 89.9°.

The LEO test cases include observations for a range of elevation angles between 5 and 88 degrees. For low elevation angles, a majority of the data, a small θ (angle between observed and computed points) implies small $\Delta\alpha$ and $\Delta\varepsilon$ so it is not surprising that the unit vector and weighted azimuth elevation representations converge to the same solution as they have the same cost function in these cases. While this finding provides no direct evidence for or against the second hypothesis it does indicate indicate the limits of where it applies. Namely that a larger percentage of higher elevation observations is needed for unit vector representation to produce a more accurate solution than weighted spherical coordinates representation. The unweighted spherical coordinates representation produced a less accurate ephemeris than the other two representations in every case. For very low elevation observations ($\cos\varepsilon \approx 1$) all three representations are equivalent but it seems that by overweighting azimuth observations at higher elevations the unweighted spherical coordinates representation uses a significantly different cost function which leads to a less accurate solution.

V.   Conclusion

In conclusion, the unit vector representation outperforms weighted and unweighted spherical coordinates representation when there are a large number of observations very close to the pole. It is both more accurate in the estimated solution and able to converge to that solution in fewer iterations. When there are few observations near the pole, unit vector representation and weighted spherical coordinates representation are equivalent in the accuracy achieved while using unweighted spherical coordinates still leads to less accurate solutions. The improvement due to the unit vector representation is due to more accurately fitting the error distribution of the observations. Therefore, the authors recommend using the unit vector representation proposed in this paper when the error in the observations is Normally and symmetrically distributed.

These results are obtained from a limited set of experimental runs with simulated data; examining a wider variety of cases would better confirm the results as well find the tipping point where the unit vector representation outperforms the other representations. Further work could be performed to characterize the effect of direction measurement representation on the estimated covariance. Additional future work could tailor a direction measurement representation to an empirical distribution derived from actual observations.

Finally, by providing quicker and more accurate OD solutions the new unit vector based direction representation can contribute to the success of a wide variety of satellite missions.

References

[1] John L. Junkins, Maruthi R. Akella, and Kyle T. Alfriend. Non-gaussian error propagation in orbital mechanics. *Astronautical Sciences*, 44(4):541–563, 1996.

[2] Oliver Montenbruck and Eberhard Gill. *Satellite Orbits: Models, Methods and Applications*. Springer, 2011.

[3] Byron D. Tapley, Bob E. Schutz, and George H. Born. *Statistical Orbit Determination*. Academic Press, 2004.

[4] John L. Crassidis and John L. Junkins. *Optimal Estimation of Dynamic Systems, Second Edition (Chapman & Hall/CRC Applied Mathematics & Nonlinear Science)*. Chapman and Hall/CRC, 2011.

[5] Richard H. Battin. *An Introduction to the Mathematics and Methods of Astrodynamics, Revised Edition (AIAA Education)*. American Institute of Aeronautics & Astronautics, 1999.

[6] David A. Vallado. *Fundamentals of Astrodynamics and Applications, 2nd. ed. (The Space Technology Library)*. Microcosm, Inc, 2001.

[7] H. K. Kuga and E. Gill. A mathematical description of the ODEM orbit determination software. DLR-GSOC IB 94-06, DLR, German Space Operations Center, 1994.

[8] A. C. Long, J. O. Cappellari, C. E. Velez, and A. J. Fuchs, editors. *Goddard Trajectory Determination System (GTDS)*. Goddard Space Flight Center, Greenbelt, MD, 1989.

[9] Mark L. Psiaki, Ryan M. Weisman, and Moriba K. Jah. Gaussian mixture approximation of the bearings-only initial orbit determination likelihood function. In *Proceedings of the AAS/AIAA Astrodynamics Specialist Conference*, 2015.

[10] G. Gaias, S. D'Amico, and J.-S. Ardaens. Angles-only navigation to a noncooperative satellite using relative orbital elements. *Journal of Guidance, Control, and Dynamics, vol. 37, issue 2, pp. 439-451*, 37(2):439–451, mar 2014.

[11] M. T. Soyka, J. W. Middour, P. W. Binning, H. Pickard, and J. Fein. The Naval Research Laboratory's Orbit/Covariance Estimation and ANalysis software - OCEAN. *Astrodynamics*, pages 1567–1586, 1997.

[12] John Parr Snyder. *Map Projections - A Working Manual*. U.S. Geological Survey, 1987.

[13] Evan M. Ward, John G. Warner, and Luc Maisonobe. Do open source tools rival heritage systems?: A comparison of tide models in ocean and orekit. In *AIAA/AAS Astrodynamics Specialist Conference, American Institute of Aeronautics and Astronautics*, 2014.